Journal of Environmental Chemical Engineering 6 (2018) 2470–2479

Contents lists available at ScienceDirect

Journal of Environmental Chemical Engineering

journal homepage: www.elsevier.com/locate/jece

Utilization of coal fly ash and drinking water sludge to remove anionic As (V), Cr(VI), Mo(VI) and Se(IV) from mine waters

Yu-Wei Chen[a], Xiao Yu[a], Emmanuel Appiah-Hagan[a], Jaime Pizarro[b], Gustavo A. Arteca[a], Louis Mercier[a], Qiliang Wei[c], Nelson Belzile[a,*]

[a] Department of Chemistry and Biochemistry, Laurentian University, Sudbury, Ontario, Canada
[b] Facultad de Ingeniería, Universidad de Santiago de ChileSantiago, Chile
[c] Centre – Energy, Materials, Telecommunications Institut national de la recherche scientifique (INRS), Varennes, Canada

ARTICLE INFO

Keywords:
Coal fly-ash
Drinking water sludge
Adsorption
Oxyanions
Mine wastewater

ABSTRACT

This study explores the potential of solid waste as effective and low-cost adsorbing materials to clean waters polluted by the mining sector. The selected adsorbents for our studies were drinking water sludge **(SLG)**, coal fly ash **(TB)** and modified fly ash **(TBFZ3)**. The adsorbates were the toxic oxyanions of As(V), Cr(VI), Mo(VI) and Se (IV). The studies were carried on in synthesized cocktail solutions **(SCS)** and real tailing pond waters **(TPW)**. The investigation revealed that both **TB** and **SLG** contain very low non-leachable impurities, thus are suitable for most waste mining water treatment. The low temperature caustic liquor treatment of fly ash **(TBFZ3)** greatly improved the adsorption properties of original **TB** and made it even cleaner. The modification technique is simple and economic compared to other processes. The solution pH influences greatly and differently the adsorption process, depending on the nature of adsorbents and adsorbates and it must be monitored and controlled carefully. Excellent adsorption capacities were observed in both **SCS** and **TPW** matrices. The adsorption kinetics and adsorption capacity of the studied materials were remarkably enhanced in the high electrolyte containing **TPW**. The adsorption generally fits well the Langmuir and Freundlich isotherms.

1. Introduction

The occurrence of toxic trace elements in natural waters and environment has drastically increased in recent decades as a consequence of industrialization and growing demand for natural resources. Wastewaters generated by the processing industries and mining sectors contain toxic metals and metalloids and must be treated at high cost to meet the guidelines established by various governmental organizations [1]. The removal of toxic elements from wastewater is usually carried out by chemical precipitation, solvent extraction, ion-exchange or adsorption. Among those, adsorption is considered as effective and low-cost in industrial processes.

In the recent years, there has been an extensive literature on the use of low-cost adsorbents to remove toxic metals and metalloids from water and wastewater. Apart from the economic advantage, the utilization of low-cost adsorbents permits the revalorization of waste or rejected materials, thus adding an environmental advantage to this approach. In the past decades, a few reviews have been published on low-cost adsorbents for wastewater treatment [2–5] as a broader topic, with some others being more specific to the nature of the materials such as coal fly-ash [6,7], cellulosic materials [8,9], plant and agricultural waste peels [10,11]. The literature on oxyanions removal from wastewater is rather limited. Among those studies, arsenic [12–16] has been investigated more than selenium [17] and chromium (VI) [18].

Coal fly ash (CFA) is an anthropogenic material obtained from coal combustion, which is predicted to increase significantly in the coming years [19]. Only a small percentage of CFA is used in concrete production, road base construction, soil amendment and zeolite synthesis; however, the large majority is still discharged into ash ponds, lagoons or landfills [19,20]. In recent years, other possible applications have been proposed including wastewater treatment [6]. The major chemical components of CFA are silica (SiO_2), alumina (Al_2O_3), calcium carbonate ($CaCO_3$) and iron oxides (Fe_2O_3) and varying amounts of carbon, sodium, magnesium and sulphur. CFA has a hydrophilic surface and it is predominantly spherical in shape with its size ranging from 0.01 TO 200 μm (an average diameter < 10 μm) and often contains irregular-shaped debris and porous un-burnt carbon [21]. Although coal contains various types of trace metals, many of them are released as gaseous form during high-temperature combustion.

The use of CFA as an adsorbent of metals and purification of mine

* Corresponding author.
E-mail address: nbelzile@laurentian.ca (N. Belzile).

https://doi.org/10.1016/j.jece.2018.03.043
Received 31 January 2018; Received in revised form 8 March 2018; Accepted 21 March 2018
Available online 28 March 2018
2213-3437/

waters has been reported by several authors (reviews previously cited). To increase its sorption kinetic and capacity, CFA is often submitted to an alkaline treatment at high temperature, thereby enhancing its active surface area, or transforming it into a synthetic zeolite-type material [22]. The alkaline nature of these modified CFA compounds usually makes them more effective in the removal of cationic metals [23–27]. It has been also reported that alkaline treated CFA has been used to adsorb phosphate after the material was treated by HCl to rend the surface positively charged [28]. A zeolite transformed from CFA was used to adsorb the metal cations (Hg, Cd, Cd, Pb) and metalloid anions (As, Se) from a simulated municipal sewage discharge [29].

Both aluminum and iron salts are used as adsorbents and coagulation-flocculation agents to adsorb and remove undesired substances from drinking water. The precipitates, drinking water sludge, together with adsorbed pollutants are removed by filtration. Very large volumes of drinking water sludge are produced daily in the world and it will become a global environmental concern as production keeps increasing [30]. Unlike CFA, drinking water sludge has even more restricted applications in the cement industry [31] or in soil remediation [32] due to the amphoteric nature of aluminum oxide. After its cleaning role in drinking water treatment, the drinking water sludge is still far below its adsorption saturation, therefore it could be still a valuable adsorbing material for contaminated waters such as industrial and mining effluents. The pH of drinking water sludge is usually slightly acidic, it might therefore be more efficient for the adsorption of anionic contaminants. Only a few authors have used this material to remove metals and oxyanions of arsenic and selenium from water solution [33–35]. They reported that adsorption of As(V) was maximum below pH 7.0 and that of Se(IV) below pH 5.0.

The specific objectives of this study were to explore the adsorption properties of CFA and drinking water sludge for four selected toxic anions (AsO_4^{3-}, SeO_3^{2-}, CrO_4^{2-}, and MoO_4^{2-}) and the parameters that influence the adsorption processes. An effort was made to find a simple, low-cost and effective procedure to improve the adsorption kinetics and capacities of these materials. The adsorption kinetics and capacities of different materials in synthesized and mine tailing-water were compared. The effect of electrolytes on adsorption kinetics and adsorption capacities are also discussed.

2. Materials and methods

2.1. Sample preparation

The CFA sample was obtained from the Thunder Bay Ontario Power Generation Plant (Canada). The sample was first dried at 50–60 °C for 24 h, then subjected to ball milling for 5 min to make the sample more homogeneous. This sample was named **TB**, and it was used without any further treatment.

A modified coal fly ash was prepared by putting 50.00 g of the sample in a 1L high density polyethylene (HDPE) bottle containing 500 mL of 2.0 mol L^1 NaOH. The material was placed in a freezer (−15 °C) first to freeze completely, then allowed to thaw in three cycles over three consecutive days to mimic Canadian climatic conditions. At the end, the liquor was removed and the material was washed many times with deionized water (DW) using centrifugation until the pH of the washing water was around 10. The material was dried at ~50 °C overnight and homogenized with a ball mill for 5 min. This sample was named **TBFZ3** and stored in a zipped bag.

The sludge collected from a discharge port of a drinking water treatment plant (City of Greater Sudbury, Canada) has a water content of 68 to 90%. The sludge was slightly acidic at around pH 5. Centrifugation was performed to collect the solid material at 4 °C at 7000 rpm for 30 min (Beckman Coulter TM). The supernatant was removed and the sludge was dried at 50 °C. The dry material **(SLG)** was homogenized with a ball mill for 5 min and stored in a zipped plastic bag.

For this study, 25L of untreated mining wastewater was collected on Oct. 26, 2015. Two 50-mL aliquots were filtered through a 0.2 µm Millipore membrane, one was acidified to 2.0%(w/w) HNO_3 for the elemental analysis by atomic adsorption/fluorescence spectroscopy and another was non-acidified for anion analysis by ionic chromatography. The **(TPW)** samples were stored in a refrigerator and analyzed shortly thereafter.

2.2. Physical and mineralogical characterization of adsorbents

The appearance of adsorbing materials was examined with scanning electron microscopy (JEOL 6400 equipped with an EDX probe Oxford X-max). The parameters such as surface area and specific pore volume of the material were determined by a particle surface analyzer with N_2 gas adsorption, and calculated based on the Brunauer-Emmett-Teller (BET) and Barrett-Joyner-Halenda (BJH) models, respectively (Micrometrics ASAP 2010, Folio Instruments). The particle size and size distribution was determined with a particle size analyzer (Microtrac S3000). The identification of crystalline phases in the materials was done using X-ray powder diffraction on a Philips PW 1820 instrument. The adsorption of As by the materials was observed by X-ray photoelectron spectroscopy (XPS, VG ESCALab 3 MARK II), using the non-monochromated AlK_α radiation (1486.7 eV). The carbon C_{1s} peak (BE = 285 eV) was used as the reference line. Data were analyzed using the Casa XPS software (2.3.15 Version) and the instrument resolution was 0.8 eV. For this analysis, a 0.50 g sample was immersed in 50.00 mL of a 400.0 mg/L As(V) solution under constant shaking (120 rpm) for 4 h. The sample was filtered and the filtrate was rejected, and the remaining solid sample was washed thoroughly with (DW). The sample was dried at 50 °C and stored for analysis.

2.3. Analytical methods in chemical characterization of adsorbents and tailing pond water

The major chemical composition of **SLG** and **TB** was measured after a sodium peroxide fusion by inductively-coupled plasma-optical-emission spectrometry in Vale Analytical Laboratories. The concentration of trace elements in **TB**, **TBFZ3** and **SLG** was obtained after an acid microwave digestion (Milestone Ethos 1600 URM) by flame or graphite atomic absorption (FAAS Analyst400 or GAAS600, Perkin Elmer) for Cr and Mo (N_2O was used as an oxidant to enhance analytical sensitivity) and by hydride generation–atomic fluorescence spectroscopy (HG–AFS, PSA 10.055 Millennium Excalibur) for As [36] and Se [37]. The same techniques were used to determine the chemical composition of **TPW**. For anion concentrations, ion chromatography (Dionex DX 500) was employed. To detect the possible leachable toxic elements from adsorbents, 0.500 g of solid was placed into a HDPE centrifuge tube with 50.0 mL of DW. The sample was submitted to a continuous horizontal shaking at 120 rpm (T = 22 ± 2 °C; pH = 7.20 ± 0.08). A 1.00-mL aliquot of liquid was pipetted at given times (4 h to 7d) and centrifuged (15000 rpm, 5 min). The supernatant was carefully taken and acidified (HNO_3 to 2%w/w) and concentrations of leachable elements were determined with GFAAS and HG–AFS.

2.4. Experimental design

2.4.1. Acid-base properties of adsorbents

The acid-base properties of the materials were investigated by soaking 0.500 g in 50.0 mL of DW or a synthesized elemental cocktail solution **(SCS)** at 50.00 mg/L of each anion, in a HDPE centrifuge tube and subjected to a constant horizontal shaking (120 rpm, 21 ± 1 °C). The pH values were periodically taken at the top supernatant solution after a centrifugation (2500 rpm, 10 min) and recorded. The pH meter was calibrated each hour with standard pH buffers. The same procedure was followed with **TPW**.

2.4.2. Adsorption at controlled pH

For this study, 0.500 g of adsorbent was placed in 50.0 mL of **SCS** at a controlled pH value. The sample was subjected to a constant horizontal shaking (120 rpm) for 4 h at 21 ± 1 °C. The pH of the mixture was monitored and adjusted to the optimal value during this period using diluted solution of NaOH or HNO_3. After 4 h, three 1.5-mL aliquots of supernatant were collected, centrifuged (15000 rpm, 5 min), acidified to 2.0% (w/w) HNO_3 and analyzed with the methods described in 2.3. The removal percentage of each element was calculated (Appendix A-Eq. S1).

2.4.3. Adsorption kinetic study

The adsorption kinetics of anions by **TB**, **TBFZ** and **SLG** was studied in both **SCS** and **TPW**. In the **SCS** matrix, 0.500 g of adsorbent was added into 50.00 mL solution at pre-adjusted pH and mixed well. At given times, two 1.50-mL aliquots of supernatant were taken and centrifuged (15000 rpm for 5 min) acidified to 2.0% (w/w) HNO_3 and stored for analysis. The pH in this study was controlled at 7.15–7.43 for the three adsorbents. In the **TPW** matrix, every step was the same, except that the solution of 50.0 mg/L of each anion was prepared in **TPW**. The pH was monitored and adjusted with 0.2 mol L^1 NaOH or 0.2 mol L^1 HNO_3 during the adsorption test and kept at a range of 7.04–7.46 for the three adsorbents. Even if the formation of hydroxides is much less problematic for element such as As and Se than it could be for divalent metals, special attention was given to the control of pH to prevent any precipitation of hydroxides instead of adsorption, especially at the beginning of the process.

2.4.4. Maximum adsorption capacity of adsorbents in both matrices and adsorption isotherm models

Single element solutions were used in this study and the optimal adsorption pH for each element determined in 2.4.2 was used. A series of different concentrations (0–410 mg/L depending on the element) of a given element were prepared in 50.00 mL of **SCS** or **TPW** matrix. A portion of 0.500 g of adsorbent was introduced into a solution with a pre-adjusted and controlled pH. The sample was shaken for 4 h until the adsorption equilibrium was reached. The sample was then centrifuged, the supernatant was collected, acidified to 2% (w/w) HNO_3 to preserve the sample and stored in a refrigerator for future analyses. The maximum adsorption capacity q_m of a given adsorbent was determined experimentally by obtaining the plateau in a plot of q_e vs C_e, where C_e (mg/L) represents the equilibrium concentration of an adsorbate in solution at a given initial concentration, q_e (mg/g) the amount of adsorbed anion at such an equilibrated system ($q_e = C_{init.} \cdot V_{init.} - C_e \cdot V_{final}$) and $q_m = \max(q_e)$. Based on these data, adsorption isotherm model fittings were performed. More detail information is given in Appendix A.

3. Results and discussion

3.1. Chemical and mineralogical characterization of adsorbents and TPW

The major element of **SLG** was Al followed by Si, Fe and other minor elements. In **TB**, Si was the dominant material, followed by Al, Ca and Fe (Appendix A-Table S1). The relatively high concentrations of Ca, Mg, Na in CFA make the material a moderate strong basic material, which is favorable for removal of Cr(VI) and Mo(VI), but less favorable for Se (IV) adsorption (see below). The XRD analyses showed that **SLG** is an amorphous material, whereas for **TB** dominant minerals include sodium aluminum silicate sulfate ($Na_8(SO_4)(Al_6Si_6O_{24})$, and $CaCO_3$, followed SiO_2. The presence of Al_2O_3 is relatively low. The mineralogy of **TBFZ3** is very similar to that of **TB**, except that the sodium aluminum silicate sulfate hydrate ($Na_{7.96}(Al_6Si_6O_{24})(SO_4)_{0.98}(H_2O)_{0.96}$) indicates clearly its presence, whereas Al_2O_3 had disappeared. This difference can be related to the modification of **TB** in a strong alkaline solution, part of $Na_8(SO_4)(Al_6Si_6O_{24}$ was hydrated, whereas some Al_2O_3 was dissolved as AlO_2^- due to its amphoteric nature. The measured concentrations of trace elements indicate that, although the concentrations of As, Cr, Mo, Se in **TB** were higher than in **SLG**, they can be considered fairly low. They were further lowered in **TBFZ3** after it had been subjected to a 2.0 mol L^1 NaOH liquor treatment, particularly for As, Se and Mo (Appendix A-Table S2). The leachability study showed that only very small amounts of trace elements (< 3 µg/L) were detected in DW after 10 days of contact, except for Se reaching 23 µg/L in **TB** sample, which indicates that leachability of trace elements can be ignored. We therefore conclude that all three materials can be considered as suitable adsorbents for mining wastewater treatment.

Table 1
Chemical composition of Vale mine tailing pond water (TPW).

Major	Na^+	K^+	Ca^{2+}	Mg^{2+}	Fe	Mn	Cl^-	SO_4^{2-}
(mg/L)	119.6	33.3	375.9	82.1	68.1	1.6	127.6	664.2

Minor	As	Cr	Mo	Se	Cd	Co	Cu	Ni	Pb
(µg/L)	1.1	7.9	0.7	1.4	5.2	349	4257	16116	6.3

Note: the concentrations of tested anions (As, Cr, Mo and Se) are expressed in µg/L of their elemental mass, not that of their respective oxyanion.

The collected **TPW** had a pH of 3.36 and a chemical composition reflecting the nature of the extracted ore (Co^{2+}, Cu^{2+} and Ni^{2+}) and oxidation of iron sulfide minerals (Table 1).

3.2. Surface characteristics of adsorbents

SLG was yellowish, amorphous and heavily aggregated in appearance. The original **TB** was composed of characteristically smooth and ball-like particles (Appendix A-Fig. S1). The 3–day freezing/thawing cycle treatment in a 2.0 mol L^1 NaOH solution has significantly increased surface areas and pore volumes of original **TB** (Table 2). **SLG** shows a much higher surface area and porosity than **TB** but both parameters were remarkably increased (~10-fold) in the modified material **TBFZ3**. **TB** has a smaller particle size compared to **TBFZ3** and **SLG** (Appendix A-Fig. S2). This is probably due to the high agglomerating nature of the last two materials which makes the particle size appearing larger.

The modification of **TB** by a caustic solution in a repeated thaw/freeze cycle has some remarkable advantages over other more energy-consuming hydrothermal modification procedures tested in the earlier stage of this work and those commonly reported in literature. With those treatments, much more energy was consumed and there was no remarkable increase in surface areas of materials and the adsorption capacity did not show a significant enhancement. The treatment with a repeated thaw/freeze cycle can use natural weather conditions to break down fly ash particles and enlarge their active surface area with a minimum energy. The process is simple and highly productive, therefore suitable for industrial process.

3.3. Acid-base properties of the materials

For adsorbents rich with ≡S−OH functional groups (≡S stands for surface composed of Si, Al, Fe, Ti hydroxide, etc.), the surface charge varies with pH. The three adsorbents showed values of pH_{pzc} above 8.0. When pH goes below the pH_{pzc} (point of zero charge), the surface becomes positively charged, thus favoring the adsorption of anions. When

Table 2
Morphological characteristics of the tested adsorbents.

Parameters (units)	SLG	TB	TBFZ3
BET surface area (m^2/g)	171.28	1.24	13.24
BJH accumulative pore volume (cm^3/g)	0.3190	0.0036	0.0345

pH increases, the negatively-charged surface becomes less favorable for anionic adsorption due to the electrostatic repulsion. **TB** and **TBFZ3** are both basic materials. In DW, the pH of **TB** solution was slightly lower than that of **TBFZ3** (10.4 vs 11.5) and both were constant in 2 h of observation. When each adsorbent was added in the **TPW** matrix without spike, the pH was 5.5 and 6.7 at first, then quickly increased to and maintained at 8.7 and 9.1, respectively. When immersing **TB** and **TBFZ3** into the **SCS** solution (pH 2.1), the pH gradually increased from 3.3 to 4.1 in 1 h, and then remained at around 4.0 for the next 6 h. The results reveal that CFA possesses a great acid neutralization capacity.

SLG is a slightly acidic material. When immersed in DW, the pH of the solution slightly decreased from 5.6 to 5.3 in 3 h. In **TPW** without spike, pH increased from 4.4 to 5.1 in 10 min, and then slowly increased to 5.3 in 4 h. However, in the more acidic **SCS** solution, the pH of **SLG** system showed a constant increase from 1.9 to 3.7 after 6 h likely due to the neutralization or adsorption of protons on the oxide/hydroxide sites of the **SLG**. This study provided useful information for pH control in later studies.

3.4. pH effect on the removal of anions in SCS

The study done in a **SCS** matrix shows that the pH influence on adsorption varies greatly depending on the nature of adsorbents and adsorbates (Fig. 1). The adsorption of the arsenate ion was the least affected by pH, which was most satisfactorily removed by all three materials in the studied pH range. **SLG** was the best material for As(V), with almost all As(V) removed under the pH range of 3.6–7.7. Although **TBFZ3** and **TB** can work over a wide pH range as **SLG**, both showed a slight drop in removal effectiveness as pH of the system increased (Fig. 1A). The modified **TBFZ3** exhibited a higher As removal efficiency in comparison to **TB** in the studied pH range. Since the arsenate ion is essentially negatively-charged over the studied pH range, it suggests that **SLG**, and to a lesser extent **TB** and **TBFZ3**, contains sufficient positive adsorbing sites to interact with arsenate ions. When the pH of a solution is lower than the pH_{pzc} of the adsorbent, positively-charged surfaces of adsorbents would be favorable to adsorption of the negatively charged $H_2AsO_4^-$ and $HAsO_4^{2-}$. The better adsorption of As(V) might also be partly due to its high affinity of Fe oxides and aluminum oxide sites [38]. As pH increases, the surface of **TB** and **TBFZ3** may become more negatively charged as they contains less ≡Al−OH and ≡Fe−OH and more ≡Si−OH sites than **SLG**. The more acidic value of pH_{pzc} of ≡Si−OH makes it less favorable for As(V) adsorption.

The adsorption of As(V) on the three selected adsorbents was confirmed by XPS analysis. The As-3p energy bonding peak clearly appeared at 144 ± 1 eV in the three adsorbents exposed to a 400 mg/L As (V) solution (Fig. 2). A comparison of the main peaks before and after adsorption is presented in Table 3.

Selenite was well adsorbed on **SLG** at a lower pH range (3.7–5.2) with a removal efficiency of 95–97% (Fig. 1D). As the pH of system increased further to ~pH 7.7, the removal dropped slightly to 85%. However, in **TB** and **TBFZ3** systems, pH drastically affected the adsorption of Se(IV) and the removal dropped from 85% to 18% as pH increased from 3.8 to 7.9 for **TBFZ3**, and from 71% to 1% as pH changed from 4.0 to 7.6 for **TB**. A possible surface charge transfer from positive to negative could explain this phenomenon. It is noticeable that with increasing pH, the same declining trend was observed in all three adsorbents, but it was more dramatic in **TB** and **TBFZ3**.

The pH influence on chromate ion adsorption was opposite to that on As and Se in **TB** and **TBFZ3** (Fig. 1B); the adsorption increased with pH, from 2.9% to 37.1% as pH increased from 3.9 to 7.6 in **TB** and from 13% to 60% as pH increased from 3.9 to 7.9 in **TBFZ3**. In the **SLG** system, pH did not appear to have any obvious effect on Cr(VI) adsorption, from pH 3.7 to 7.7 as its removal% was relatively stable at 45.5–48.8%. For the molybdate ion (MoO_4^{2-}), an increase in pH also promoted adsorption on all three materials (Fig. 1C), but with a lesser degree in **SLG**. Increasing pH from 3.9 to 7.9 made the removal% of Mo

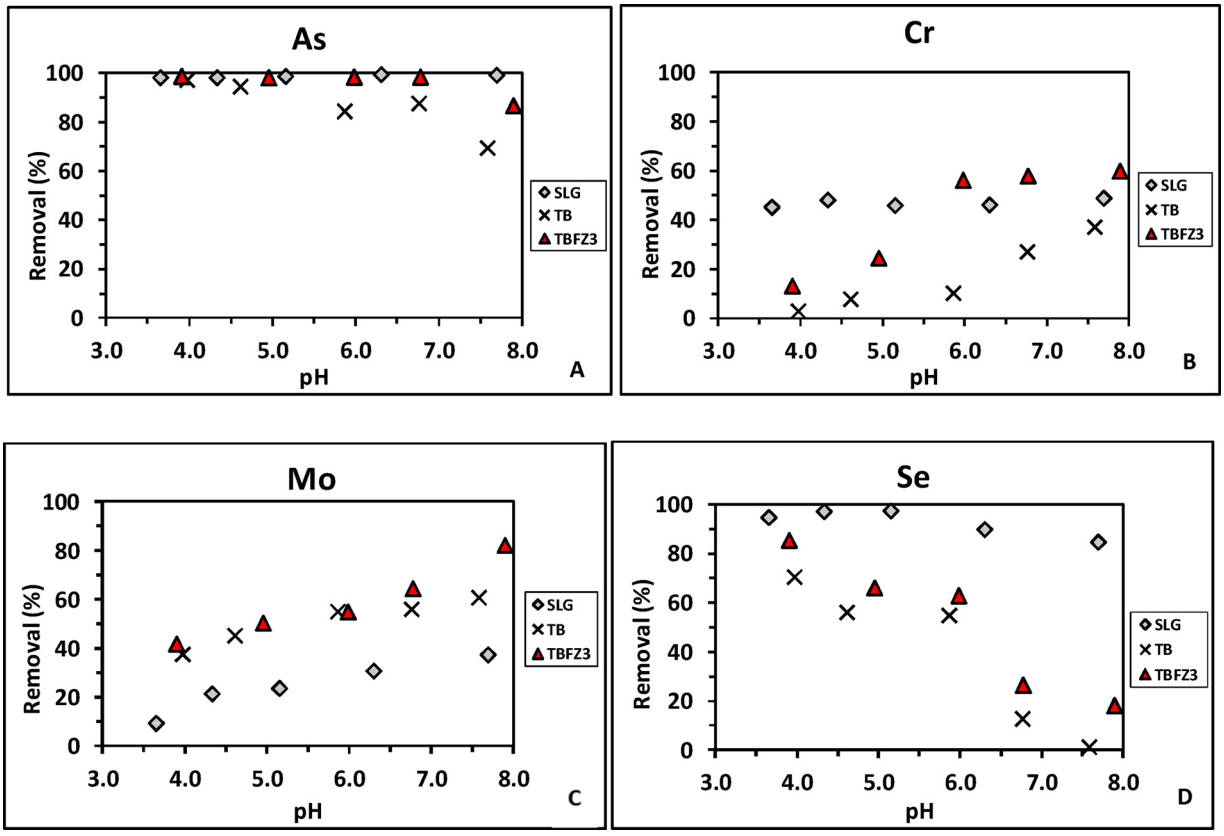

Fig. 1. Effect of solution pH on the removal efficiency of anionic species. For details, refer to Section 2.4.2.

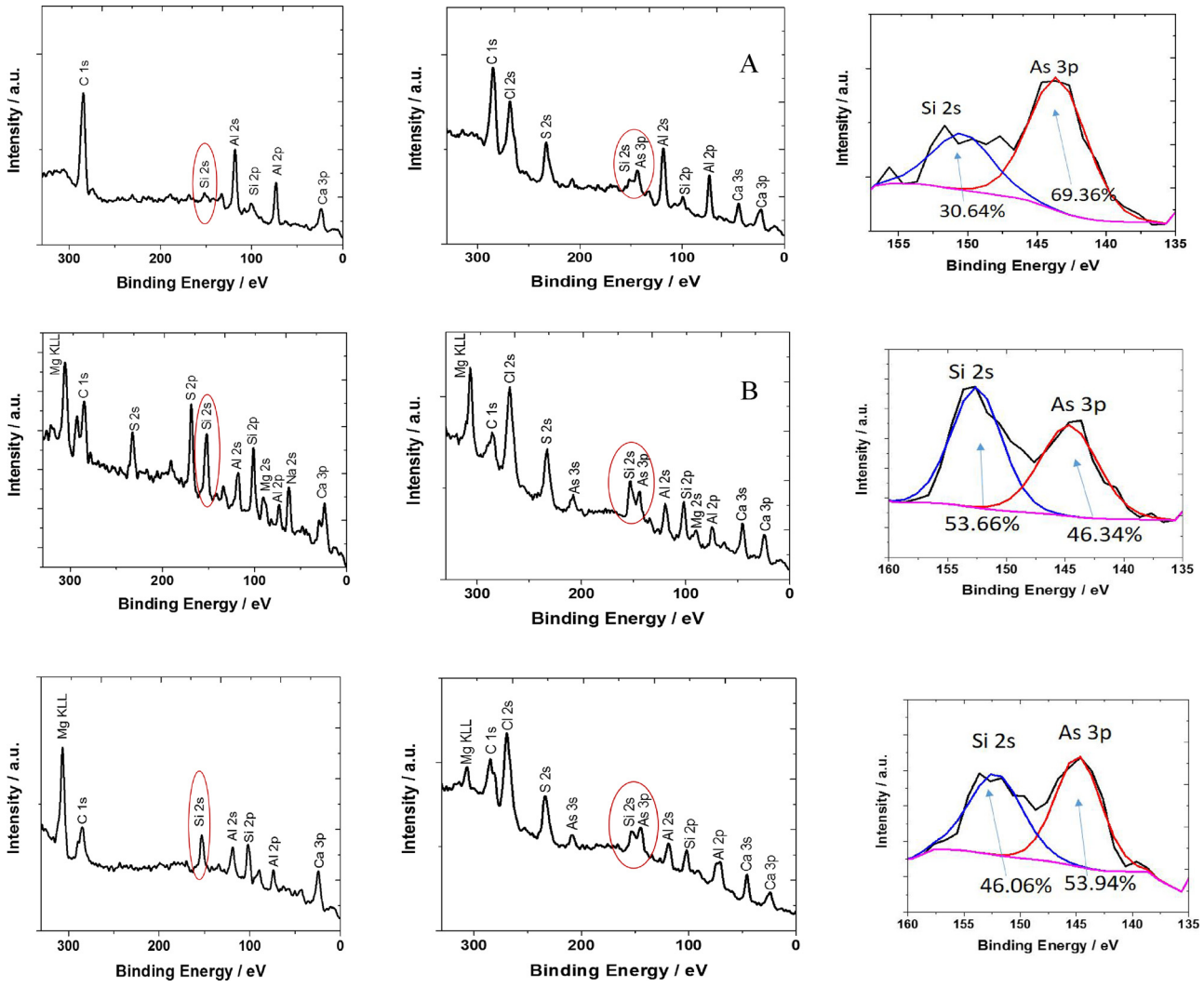

Fig. 2. High resolution XPS spectra showing the As-3p peak partially overlapping with that of Si-2p on sample SLG (A), TB (B) and TBFZ3 (C). No As-3p peak appeared on the control samples (left panels).

Table 3
Major peaks of XPS analysis before and after As adsorption.

Adsorbent	Element	Position before (eV)	Position after (eV)
SLG	O 1s	532	532
	C 1s	285	285
	Al 2p	73	74
	Si 2p	100	100
	As 3p	–	143
TB	O 1s	531	531
	C 1s	285	285
	Ca 2p	348	347
	Al 2p	74	74
	Si 2p	102	101
	S 2p	169	169
	As 3p	–	145
TBFZ3	O 1s	532	532
	C 1s	285	285
	Ca 2p	348	343
	Al 2p	75	71
	Si 2p	103	102
	Mg 2s	90	90
	As 3p	–	145

(VI) enhanced from 42% to 82% for **TBFZ3** and 38% to 61% for **TB** respectively. **SLG** was the less effective adsorbent and could only remove 37% of Mo(VI) at pH 7.7 in the **SCS** matrix.

These results suggest that the adsorption mechanism may be very different for different adsorbents and different adsorbates. In the case of As and Se, the surface charge with the increase of pH either affects very little the efficiency of element removal (in the case of **SLG**), or decreases it markedly (in the case of Se in **TB** and **TBFZ3**). On the other hand, the process of removal was enhanced to some extent for Cr and Mo, except for Cr in **SLG**, where there was no effect. The data are not sufficient to propose a different mechanism, but some possibilities might be conjectured. For instance, at low pH Cr(VI) and Mo(VI) can form large polyoxometalate species (e.g., $Cr_3O_{10}^{2-}$, $Mo_2O_7^{2-}$, etc.). Whereas the low solubility of these species may enhance their retention by some adsorbents, their large size may render them more difficult to remove when using some other adsorbent materials. The high pH may favour their release from the matrix [39]. On the other hand, the uptake of Mo(VI) by organic matrices is known to be maximized at low pH [40], thereby suggesting that the mechanism is strongly dependent on the nature of the adsorbent's surface. In contrast, As(V) and Se(IV) show different behaviors, where the formation of polyarsenic and polyselenic compounds is not favoured.

It is worth mentioning that none of the four oxyanions formed precipitates in the tested pH range of 3.6–7.9, which confirms that any removal of these elements from solution was due to surface adsorption. This experiment indicates the crucial importance of pH in adsorption studies, which is not always well investigated in previous literature.

3.5. Adsorption properties of the materials

In earlier studies, we had attempted to modify a mixture of **TB** and **SLG** by refluxing it in 2.0 mol L^{1} NaOH liquor at high temperature (150 °C for 4 h). It failed because the high dissolution of aluminum oxide in **SLG** under such conditions. The product of such treatment showed much reduced adsorption properties towards the studied oxyanions compared to **SLG** and fly-ash alone. The simple mechanical mixing of both materials (e.g. 4SLG:1TB − SLG:4TB) did not show any significant advantage, hence no further investigation in that direction was pursued.

3.5.1. Adsorption kinetics of oxyanions in SCS and TPW

Many factors can affect the adsorption kinetics of ions on porous solid surfaces. The transfer in the solution is controlled by the diffusion rate which is in turn related to the charge and size of the ion and the complexity of the solution and its pH and to the transport from the external surface to intra-particle sites. The nature of the surface is also important in terms of surface area and specific affinities with some ions for the surface and functionalities. The adsorption kinetics of the four anions on the three adsorbents were first carried out in the **SCS** matrix (50.00 mg/L each). Based on the previous pH effect study, a compromise pH for the cocktail anions system was controlled at 7.00–7.50, although in this given pH range the adsorption of Se(IV) on **TB** and **TBFZ3** was low. In **SCS**, the adsorption kinetics and completeness varied greatly between different adsorbates and adsorbents. On **SLG** (pH 7.15 ± 0.19), adsorption equilibrium of As was achieved in 2 h with a 98% removal (Fig. 3A). Although it was not complete, Se removal gradually reached nearly 80% (Fig. 3D). For Mo, an equilibrium was reached in 4 h with a 51% removal (Fig. 3C), whereas that of Cr was 47% after 7 h (Fig. 3B). On **TBFZ3** at pH 7.31 ± 0.34 and **TB** at pH 7.45 ± 0.35, Mo appeared to be achieving equilibrium much faster than As and Cr, and the adsorption kinetics of the latter two elements in **TB** and **TBFZ3** were slower and removal% lower than in **SLG**. In close, the adsorption of Cr(VI) was less satisfactory than the other three anions in **SCS**. For Mo(VI), the adsorption of Mo by **TBFZ3** appeared instantaneous and complete, and to a lesser degree by **TB**. The adsorption of As(V) in **SLG** was fast and complete in a very wide pH range. **SLG** can adsorb Se well with a good rate at the testing pH, but not **TBFZ3** and **TB**. It was also noticed that **TBFZ3** demonstrated a significant advantage over **TB** in all studied anions. Points in figures are the average values of triplicates.

Kinetic studies were also conducted in a cocktail solution at 10, 30, 60, 90, 120, 180 and 240 min contact time, prepared in **TPW** where high concentrations of sulfate and other ions were present (Fig. 4). Although TPW contained high concentrations of Cu, Ni, Co (Table 1), the concentrations of studied anions were much lower than those of spiked anions (50.0 mg/L each), thus the original concentrations of the studied anions in **TPW** was ignored. To facilitate the comparison, the pH conditions were kept very close in both studies with **SCS** and **TPW** matrices.

In **TPW**, the adsorption of As(V) was instantly completed on all three materials, in comparison to a relatively slow kinetics in **SLG** and slow and incomplete adsorption in **TBFZ3** and **TB** in **SCS**. For Se, unlike in **SCS** where the adsorption of Se(IV) on **TB** and **TBFZ3** was zero or negligible, the adsorption of Se(IV) on the three materials in **TPW** was as rapid and complete as for As(V) in the same matrix. In **TPW**, the adsorption of Mo(VI) and Cr(VI) decreased slowly in all three adsorbents compared to those in **SCS**.

The adsorption rates of the four anions on SLG TB and TBFZ3 were investigated by the Lagergren pseudo-first order Eq. (1) and pseudo-second order Eq. (2) models [41]:

$$\ln(q_e - q_t) = \ln(q_e) - k_1 t \quad (1)$$

$$\frac{t}{q_t} = \left(\frac{t}{q_e}\right) + \frac{1}{k_2 q_e^2} \quad (2)$$

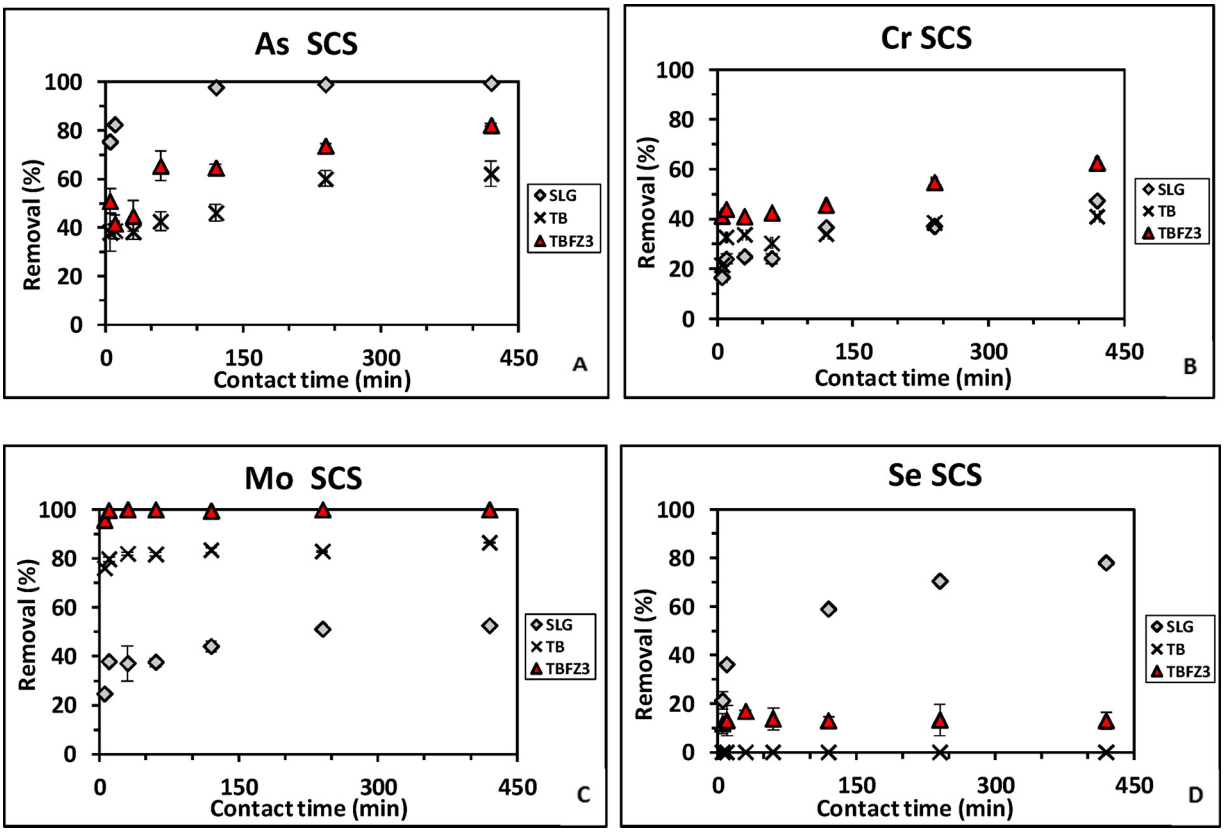

Fig. 3. Adsorption kinetics of the four anions in the SCS matrix. For details, refer to Section 2.4.3.

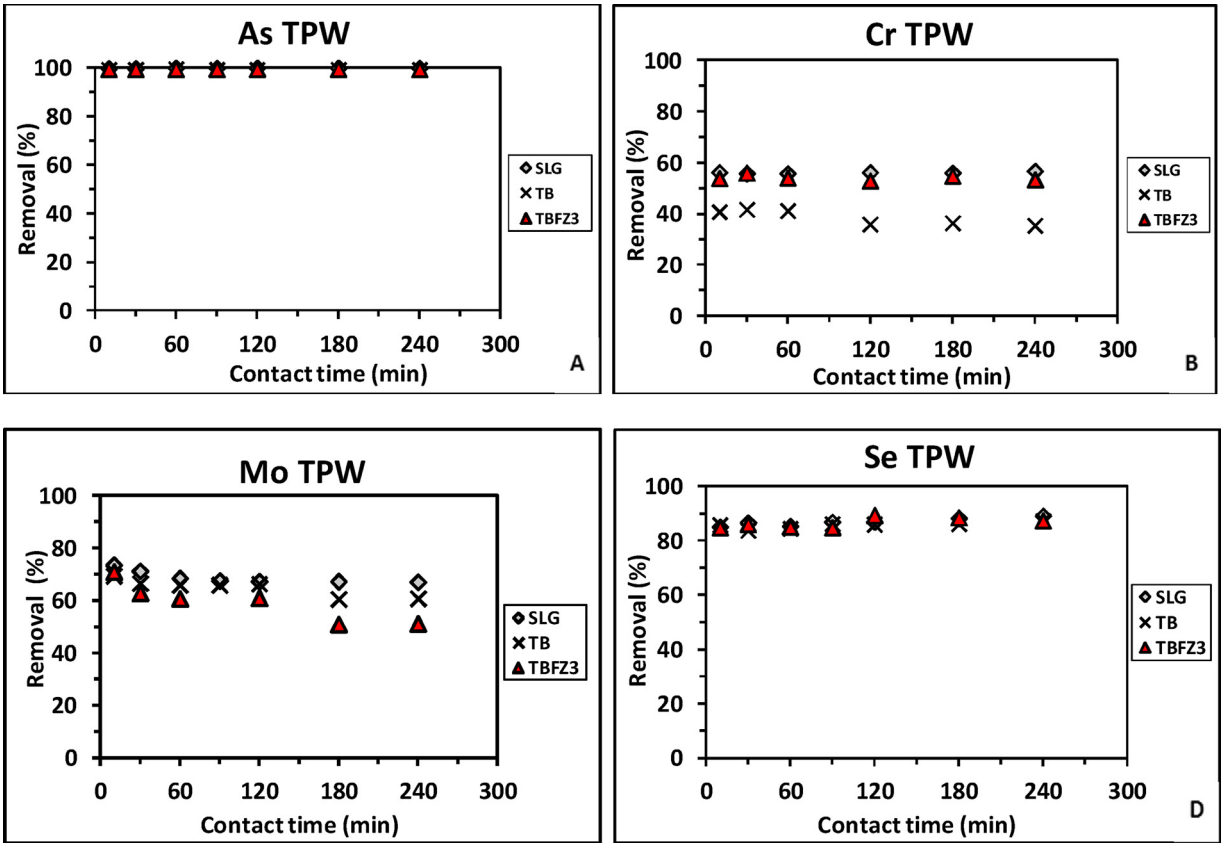

Fig. 4. Adsorption kinetics of the four anions in the TPW matrix. For details, refer to Section 2.4.3.

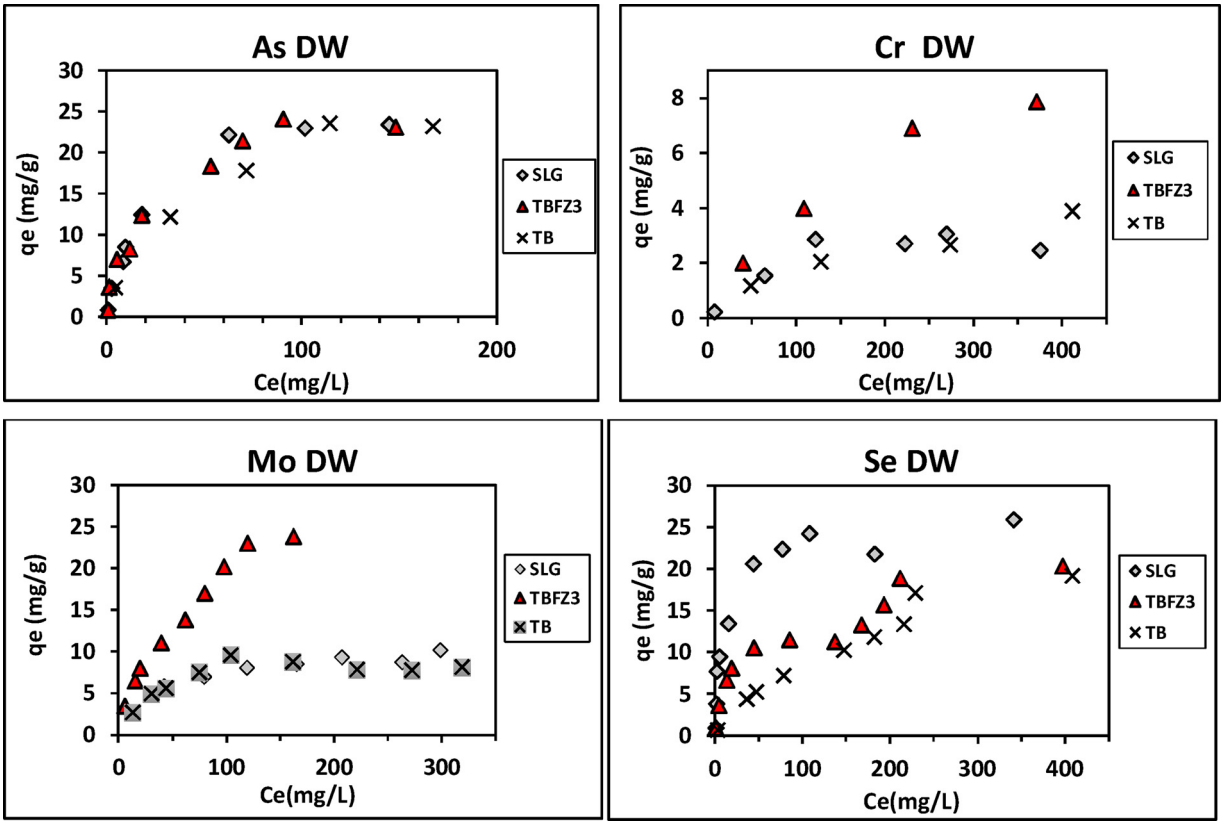

Fig. 5. Adsorption isotherms of anions in the SCS matrix. The pH was controlled at 7.29 ± 0.07, 7.12 ± 0.06, 7.19 ± 0.04 and 5.21 ± 0.04 for As(V), Cr(IV), Mo (VI) and Se(IV), respectively, and presented as an average of pH performed in three tested materials. For other details, refer to Section 2.4.4.

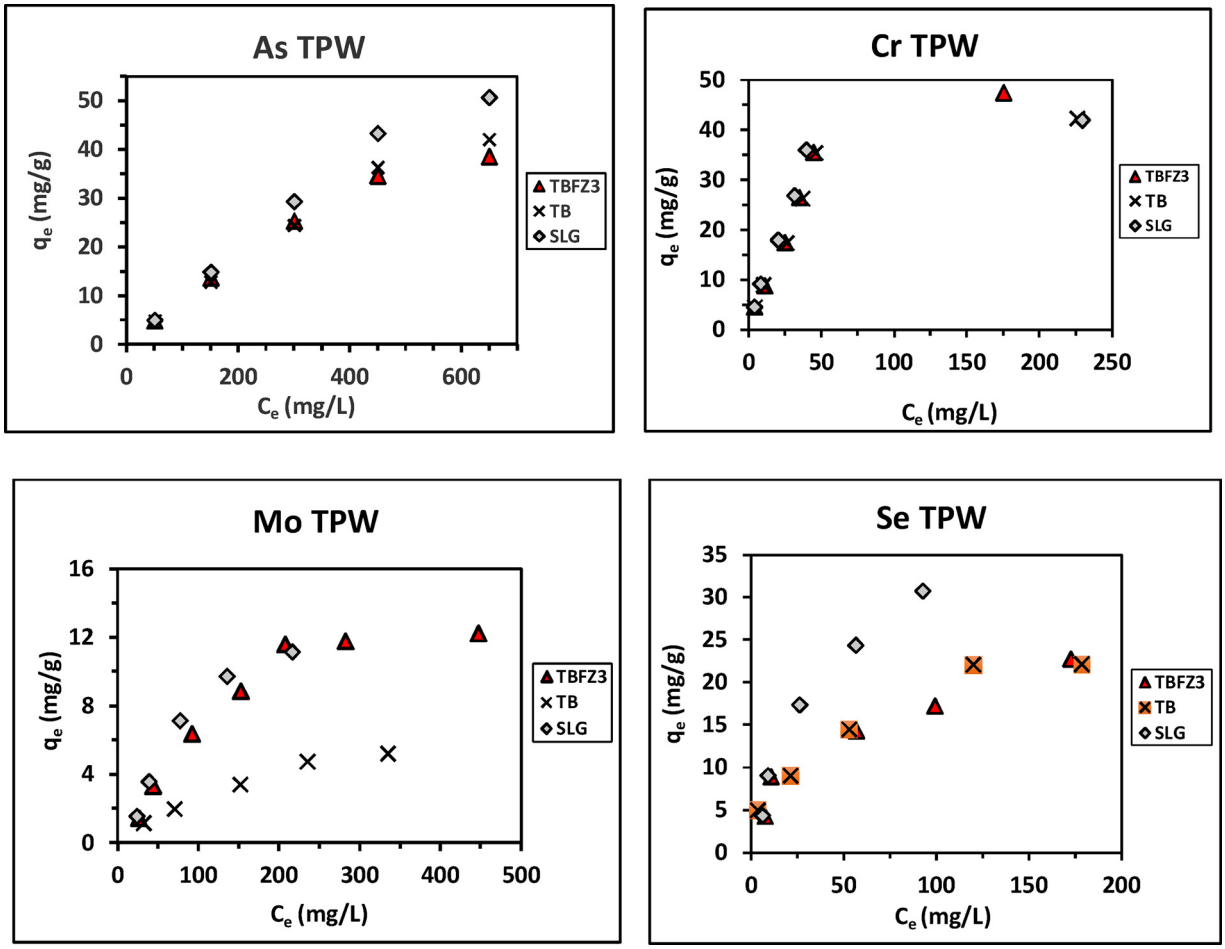

Fig. 6. Adsorption isotherms of anions the TPW matrix. The pH was controlled at 7.14 ± 0.06, 7.21 ± 0.11, 7.23 ± 0.11 and 5.14 ± 0.08 for As(V), Cr(IV), Mo (VI) and Se(IV), respectively, and presented as an average of pH performed in three tested materials. For other details, refer to Section 2.4.4.

Table 4
Comparison of q_{mcalc} from Langmuir fitting model and $q_{mexp.}$ from isotherms.

	SCS						TPW					
	q_{mcalc} (mg/g)			q_{mexp} (mg/g)			q_{mcalc} (mg/g)			q_{mexp} (mg/g)		
	SLG	TB	TBFZ3	SLG	TB	TBFZ3	SLG	TB	TBFZ3	SLG	TB	TBFZ3
As(V)	26.6	28.9	25.6	23.5	23.6	24.2	52.1	48.5	42.0	50.8	42.1	38.6
Cr(VI)	3.2	5.4	12.5	3.1	4.0	9.1	46.7	49.0	62.9	41.3	41.7	47.5
Mo(VI	10.8	8.6	33.2	10.2	8.2	23.8	24.9	17.9	39.1	11.2	10.4	27.3
Se(IV)	25.8	29.9	20.5	25.9	19.2	20.3	49.8	27.8	27.2	32.9	24.6	28.5

where q_t is the adsorption at time t, q_e is the adsorption capacity at adsorption equilibrium and k_1 and k_2 are the kinetic rate constants for the pseudo-first order and pseudo-second order models, respectively. The kinetic adsorption data were fitted to both equations and the results did not fit well with Lagergren pseudo first–order model but fit much better to Eq. (2) with R^2 of 0.973–1.000 for all adsorbents (Appendix A-Table S5). The pseudo-second order model has been explained by the overall adsorption rate being limited by the rate of the ion diffusion in the pore of the adsorbent also called the intraparticle diffusion model [42].

3.5.2. Adsorption isotherms and adsorption capacity of the materials

This set of studies were conducted in a single adsorbate solution in both **SCS** and **TPW**. All adsorption isotherms were performed at optimal pH of each system. Isotherms in **SCS** and **TPW** matrices are presented in Figs. 5 and 6.

The Langmuir model is based on the hypotheses that (1) at a constant temperature, all sites possess the same capacity of adsorption (homogeneous adsorption system), (2) there is no interaction between adsorbed molecules with molecules on adjacent sites and (3) each adsorption site can adsorb only one molecule, meaning the adsorption is monolayer [43]. The mechanism comprises three steps with rate constant k_1, a reversible desorption with rate constant k_{-1}, and a "reaction-on-surface" step with rate constant k_2 (Appendix A-Eq. S2). It was initially developed with an adsorption system of a solid phase to gaseous molecules, but later it has been also applied to a solid and liquid system (Appendix A-Eqs. S3–S4). It was used here to compare the calculated and experimental values of $q_{m.}$ Similarly, the Freundlich isotherm was first derived as an empirical equation to express the correlation between the concentration of a solute on the surface of a solid adsorbent and its concentration in the liquid phase of an adsorption system under an isotherm condition. It was later extended to a heterogeneous surface

and multilayer adsorption system (Appendix A-Eq. S5). In general, the Langmuir model fits better than the Freundlich model thereby suggesting that the adsorption is the result of a strong chemical interaction with the surface, leading to a monolayer (Appendix A-Table S4).

In **SCS**, the q_m of all three tested materials for As(V) were all very high and were the opposite for Cr(VI). The q_m of **SLG** for Se was very close to that of As(V), whereas that of **TB** and **TBFZ3** were slightly lower. For Mo(VI), the q_m of **TBFZ3** was more than 2 times higher than that of **SLG** and **TB** (Table 4). When experiments were conducted in **TPW**, not only the adsorption kinetics was increased, but also the q_m of oxyanions for Se(IV), more for As(V) and slightly for Mo(VI). The most striking increase was with Cr(VI), where the q_m values increased by more than 13, 10 and 5 times for **SLG**, **TB** and **TBFZ3**, respectively (Table 4).

The comparison of q_m between the values extracted directly from isotherm plateau (q_{mexp}) and those calculated that are based on the Langmuir fitting (q_{mcalc}) generally agree well with each other. It is also noticed that q_{mexp} values are generally lower than q_{mcalc} values. It is somehow expected since the former values are obtained based on the highest point of an isotherm plateau which often did not yet reach complete adsorption saturation due to the limitations in the experimental design.

4. Conclusion

Drinking water sludge and coal fly ash contain rich and valuable adsorption materials such as oxides of Al, Fe, Si, Ca and Mg. Although considered as industrial waste materials, they are clean and suitable to be used in mine wastewaters treatment at low or no cost. **SLG** is a porous material with high surface area. Fly ash modification performed in a re-usable alkaline liquor at a low temperature is a simple, energy-saving and easily-applicable for industrial processing. The surface area of the so-modified fly ash has been improved by 11-fold and the pore volume by 10. The adsorption kinetics and capacities of fly ash were generally increased after modification.

The adsorption of oxyanions is strongly influenced by pH solutions. Although As can be adsorbed by **SLG** in a wide pH range, pH should be controlled between 5.5 and 8.0 to avoid dissolution of the material at lower and higher pH due to the amphoteric properties of Al oxides. A higher pH reduced the adsorption of Se(IV) on both **TB** and **TBFZ3** and promoted the adsorption of Cr(VI) and Mo(VI) on these two materials.

In the SCS system at pH 7.3 ± 0.3, **SLG** showed the fastest adsorption rate for As(V), with 97.0% of the anion removed from the aqueous phase within 2 h. The removal% was lower for Se(IV), Mo(VI) and Cr(VI) with 78.0, 52.7 and 41.0%, respectively after 7 h. **TBFZ3** was more effective than **TB** in removing As(V), Cr(VI) and Mo(VI). In **TPW**, the adsorption kinetics and completeness of As and Se on the three tested materials have been remarkably increased, particularly for Se on **TB** and **TBFZ3** from almost zero to 100% in a few minutes. In addition, compared to the **SCS** matrix, the adsorption capacities of materials (q_{mexp}) in **TPW** all increased except only in a few cases, and the most remarkable increase was observed with Cr(VI) where q_{mexp} increased by 13, 10 and 5 times and reached 41.3, 41.7 and 47.5 mg/g for **SLG**, **TB** and **TBFZ3**, respectively.

In conclusion, all three materials can most effectively adsorb As in a wide pH range; fly ash and modified fly ash can adsorb Se and Mo to a satisfactory degree in an optimal pH. Matrix **TPW** with a high electrolyte content greatly enhanced the adsorption of all elements, particularly Cr(IV). The proposed fly ash modification is simple and cost-effective compared with many other procedures. The adsorption isotherms usually fitted better to the Langmuir model than to the Freundlich model. The used materials could potentially be desorbed and reused or disposed of in tailing ponds.

Acknowledgements

The research was financially supported by the Natural Sciences and Engineering Research Council of Canada with its Research Partnerships Programs, Vale Canada Ltd and Laurentian University.

Appendix A. Supplementary data

Supplementary data associated with this article can be found, in the online version, at https://doi.org/10.1016/j.jece.2018.03.043.

References

[1] WHO, Guidelines for Drinking-water Quality, World Health Organization, 2011 564 pp http://www.who.int/water_sanitation_health/publications/2011/dwq_guidelines/en/.
[2] M. Ahmaruzzaman, Industrial wastes as low-cost potential adsorbents for the treatment of wastewater laden with heavy metals, Adv. Colloid Interf. Sci. 166 (2011) 36–59.
[3] S. Babel, T.A. Kurniawan, Low-cost adsorbents for heavy metals uptake from contaminated water; a review, J. Hazard. Mater. 7 (2003) 219–243.
[4] V.K. Gupta, P.J.M. Carrott, M.M.L. Ribeiro Carrott, Suhas, Low-cost adsorbents: growing approach to wastewater treatment –a review, Crit. Rev. Environ. Sci. Technol. 39 (2009) 783–842.
[5] E. Iakovleva, M. Sillanpää, The use of low-cost adsorbents for wastewater purification in mining industries, Environ. Sci. Pollut. Res. 20 (2013) 7878–7899.
[6] M. Ahmaruzzaman, A review on the utilization of fly ash, Progr. Energ. Combust. 36 (2010) 327–363.
[7] S. Wang, H. Wu, Environmental-benign utilization of fly ash as low-cost adsorbents, J. Hazard. Mater. B 136 (2006) 482–501.
[8] S. Hokkanen, A. Bhatnagar, M. Sillanpää, A review on modification methods to cellulose-based adsorbents to improve adsorption capacity, Water Res. 91 (2016) 156–173.
[9] D.S. Malik, C.K. Jain, A.K. Yadav, Removal of heavy metals from emerging cellulosic low-cost adsorbents: a review, Appl. Water Sci. (2016) 2113–2136, http://dx.doi.org/10.1007/s13201-016-0401-8.
[10] A. Bhatnagar, M. Sillanpää, A. Witek-Krowiak, Agricultural waste peels as versatile biomass for water purification – a review, Chem. Eng. J. 270 (2015) 244–271.
[11] W.S. Wan Ngah, M.A.K.M. Hanafiah, Removal of heavy metal ions from wastewater by chemically modified plant wastes as adsorbents: a review, Bioresour. Technol. 99 (2008) 3935–3948.
[12] A. Dadwal, V. Mishra, Review on biosorption of arsenic from contaminated water, Clean Soil Air Water 45 (2017) 1600364.
[13] D. Kumar, V. Tomar, New generation material for the removal of arsenic from water, in: A. Tiwati, M. Syväjärvi (Eds.), Advanced Materials for Agriculture, Food, and Environmental Safety, Scrivener Publ., 2014, pp. 61–85.
[14] D. Mohan, C.U. Pittman Jr., Arsenic removal from water/wastewater using adsorbents – a critical review, J. Hazard. Mater. 142 (2007) 1–53.
[15] M.K. Mondal, R. Garg, A comprehensive review on removal of arsenic using activated carbon prepared from easily available waste materials, Environ. Sci. Pollut. Res. (2017) 13295–13306, http://dx.doi.org/10.1007/s11356-017-8842-7.
[16] G. Ungureanu, S. Santos, R. Bonaventura, C. Botelho, Arsenic and antimony in water and wastewater: overview of removal techniques with special reference to latest advances in adsorption, J. Environ. Manage. 151 (2015) 326–342.
[17] S. Santos, G. Ungureanu, R. Boaventura, C. Botelho, Selenium contaminated waters: an overview of analytical methods: treatment options and recent advances in sorption methods, Sci. Total Environ. 521–522 (2015) 246–260.
[18] K. Mukherjee, R. Saha, A. Ghosh, B. Saha, Chromium removal technology, Res. Chem. Intermed. 39 (2013) 2267–2286.
[19] Z.T. Yao, Y.S. Ji, P.K. Sarker, J.H. Tang, L.Q. Ge, M.S. Xia, Q. Xi, A comprehensive review on the applications of coal fly ash, Earth-Sci. Rev. 141 (2015) 105–121.
[20] H. Cho, D. Oh, K. Kim, A study on removal characteristics of heavy metals from aqueous solution by fly ash, J. Hazard. Mater. B127 (2005) 187–195.
[21] S.F. Ghosal, S.A. Self, Particle size-density relation and cenosphere content of coal fly ash, Fuel 74 (1995) 522–529.
[22] H. Höller, U. Wirsching, Zeolite formation from fly ash, Forschr. Miner. 63 (1985) 21–43.
[23] K.S. Hui, C.Y.H. Chao, S.C. Kot, Removal of mixed heavy metals ions in wastewater by zeolite 4A and residual products from recycled coal fly ash, J. Hazard. Mater. B127 (2005) 89–101.
[24] N. Moreno, X. Querol, C. Ayora, C.F. Pereira, M. Janssen-Jurkocicová, Utilization of zeolites synthetized from coal fly ash for the purification of acid mine waters, Environ. Sci. Technol. 35 (2001) 3526–3534.
[25] P.K. Sahoo, S. Tripathy, M.K. Panigrahi, Sk.Md. Equeenuddin, Evaluation of the use of an alkali modified fly ash as a potential adsorbent for the removal of metals from acid mine drainage, Appl. Water Sci. 3 (2013) 567–576.
[26] M. Visa, A.M. Chelaru, Hydrothermally modified fly ash for heavy metals and dyes removal in advanced wastewater treatment, Appl. Surf. Sci. 303 (2014) 14–22.
[27] C. Wang, J. Li, X. Sun, L. Wang, X. Sun, Evaluation of zeolites synthesized from fly ash as potential adsorbents for wastewater containing heavy metals, J. Environ. Sci. 21 (2009) 127–136.
[28] P. Pengthamkeerati, T. Satapanajaru, P. Chularuegoaksorn, Chemical modification

of coal fly ash for the removal of phosphate from aqueous solution, Fuel 87 (2008) 2469–2476.
[29] J. Xie, Z. Wang, D. Wu, H. Kong, Synthesis and properties of zeolite/hydrated iron oxide composite from coal fly ash as efficient adsorbent to simultaneously retain cationic and anionic pollutants from water, Fuel 116 (2014) 71–76.
[30] T. Okuda, W. Nishijima, M. Sugimoto, N. Saka, S. Nakai, K. Tanabe, J. Ito, K. Takenaka, M. Okada, Removal of coagulant aluminum from water treatment residuals by acid, Water Res. 60 (2014) 75–81.
[31] N.H. Rodríguez, S. MartínezRamírez, M.T. Blanco Varela, M. Guillem, J. Puig, E. Larrotcha, J. Flores, Re-use of drinking water treatment plant (DWTP) sludge: characterization and technological behaviour of cement mortars with atomized sludge additions, Cem. Concr. Res. 40 (2010) 778–786.
[32] K.C. Makris, W.G. Harris, Time dependency and irreversibility of water desorption by drinking water treatment residuals: implication for sorption mechanisms, J. Colloid Interf. Sci. 294 (2005) 151–154.
[33] Y.-F. Zhou, R.J. Haynes, Removal of Pb(II), Cr(III) and Cr(VI) from aqueous solutions using alum-derived water treatment sludge, Water Air Soil Pollut. 215 (2011) 631–643.
[34] Y.-F. Zhou, R.J. Haynes, A comparison of inorganic solid wastes as adsorbents of heavy metal cations in aqueous solution and their capacity for desorption and regeneration, Water Air Soil Pollut. 218 (2011) 457–470.
[35] Y.-F. Zhou, R.J. Haynes, A comparison of water treatment sludge and red mud as adsorbents of As and Se in aqueous solution and their capacity for desorption and regeneration, Water Air Soil Pollut. 223 (2012) 5563–5573.
[36] L.S. Cutter, G.A. Cutter, M.L.C. San Diego-McGlones, Simultaneous determination of inorganic arsenic and antimony species in natural waters using selective hydride generation with gas chromatography/photoionization detection, Anal. Chem. 63 (1991) 1138–1142.
[37] Y.-C. Chen, X.-L. Zhou, J. Tong, T.H.Y. Truong, N. Belzile, Photochemical behavior of inorganic and organic selenium compounds in various aqueous solutions, Anal. Chim. Acta 545 (2005) 149–157.
[38] N. Belzile, A. Tessier, Interactions between arsenic and iron oxyhydroxides in lacustrine sediments, Geochim. Cosmochim. Acta 54 (1990) 103–109.
[39] I. Thornton, Geochemical aspects of the distribution and forms of heavy metals in soils, in: N.W. Lepp (Ed.), Effect of Heavy Metal Pollution in the Environment, Applied Science Publ., London, 1981, pp. 1–33.
[40] P.L.G. Vlek, W.L. Lindsay, Thermodynamic stability and solubility of molybdenum minerals in soils, Soil Sci. Soc. Am. J. 41 (1977) 42–46.
[41] Y.S. Ho, G. McKay, Pseudo-second order model for sorption processes, Process Biochem. 34 (1999) 451–465.
[42] W. Plazinski, J. Dziuba, W. Rudzinski, Modeling of sorption kinetics: the pseudo-order equation and sorbate intraparticle diffusivity, Adsorption 19 (2013) 1055–1064.
[43] R. Masel, Principles of Adsorption and Reaction on Solid Surfaces, Wiley Interscience, 1996, pp. 235–353.